Dalton Transactions

PAPER

Application of hydrophobically modified water-soluble polymers for the dispersion of hydrophobic magnetic nanoparticles in aqueous media†

Cite this: *Dalton Trans.*, 2014, **43**, 8633

Zacharoula Iatridi,[a] Violetta Georgiadou,[b] Melita Menelaou,[b] Catherine Dendrinou-Samara*[b] and Georgios Bokias*[a]

Hydrophobically modified water-soluble polymers (HMWSPs), comprised of a poly(sodium methacrylate) (PMANa) or poly(sodium acrylate) (PANa) backbone and pendent dodecyl methacrylate (DMA) or dodecyl acrylamide (DAAm) chains, respectively, were synthesized. The hydrophobic content of the copolymers, P(MANa-co-DMA) and P(ANa-co-DAAm), is in the range of 0 to 25 mol%, while their weight-average molar mass varies from ~10 000 up to ~75 000. Their self-assembly behavior in dilute aqueous solution was followed through Nile Red probing, DLS and TEM measurements. The critical micelle concentration (CMC) is mainly controlled by the hydrophobic content and not the molar mass of the copolymers. Above CMC, spherical and large-compound micelles are identified by DLS and TEM. Moreover, oleylamine coated $CoFe_2O_4$ nanoparticles ($CoFe_2O_4$@OAm MNPs) of 9.4 nm with a saturation magnetization M_s = 85 emu g^{-1} were solvothermally prepared. The hydrophobic $CoFe_2O_4$@OAm MNPs were successfully encapsulated into the hydrophobic cores of the structures formed by the copolymers above CMC through a solvent mixing procedure, and in that way hydrophilic $CoFe_2O_4$@HMWSP nanohybrids resulted. For comparison purposes, two alternate phase transfer approaches were also used to convert $CoFe_2O_4$@OAm MNPs to hydrophilic ones: (a) addition of a coating layer by cetyltrimethyl ammonium bromide (CTAB) and (b) by the ligand exchange procedure with 2,3-dimercaptosuccinic acid (DMSA). NMR transverse relaxivity measurements of the aqueous suspensions of $CoFe_2O_4$@P(ANa-co-DAAm), $CoFe_2O_4$@CTAB and $CoFe_2O_4$@DMSA were recorded and the r_2 relaxivity was determined. $CoFe_2O_4$@CTAB demonstrated the highest r_2 relaxivity of 554.0 mM^{-1} s^{-1}, while $CoFe_2O_4$@P(ANa-co-DAAm) and $CoFe_2O_4$@DMSA showed lower values of 313.6 mM^{-1} s^{-1} and 76.3 mM^{-1} s^{-1}, respectively.

Received 6th February 2014,
Accepted 26th March 2014

DOI: 10.1039/c4dt00393d

www.rsc.org/dalton

Introduction

The self-assembly behavior of amphiphilic copolymers in aqueous media has been a very attractive topic for decades as they find use in numerous applications like drug delivery systems, cosmetics, paints, colloids, emulsifiers, coatings and rheology modifiers.[1] The leading forces for self-association of amphiphilic polymer chains are hydrophobic interactions along with intramicellar electrostatic interactions. In the case of amphiphilic polyelectrolytes, hydrophobic monomer units and hydrophilic electrolyte monomer units are attached on the same polymer chain. While amphiphilic block copolymers have been extensively investigated,[1b–d,2] the self-assembly of random amphiphilic copolymers is becoming more and more intriguing. Numerous scientific groups have reported a variety of morphologies[3] of random amphiphilic copolymer self-assemblies like spherical micelles, flower-like micelles, large-compound or multicore micelles, vesicles, *etc.*

Random amphiphilic copolymers can be either linear, consisting of small hydrophilic and hydrophobic units, or of a comb-like structure, consisting of a hydrophilic backbone (for example, poly(sodium acrylate),[4] polyacrylamide[5] or natural derivatives[6]) and long alkyl hydrophobic pendent chains (typically, dodecyl- or octadecyl-chains). This latter class is usually called hydrophobically modified water-soluble polymers (HMWSP)[7] and has been extensively studied and proposed for applications such as rheology modifiers, emulsion stabilizers, *etc.*[8]

[a]*Department of Chemistry, University of Patras, GR-26504 Patras, Greece. E-mail: bokias@upatras.gr; Fax: (+30) 2610-997122; Tel: (+30) 2610-997102*
[b]*Department of Chemistry, Aristotle University of Thessaloniki, GR-54124 Thessaloniki, Greece. E-mail: samkat@chem.auth.gr; Fax: (+30) 2310-997876; Tel: (+30) 2310-997876*

† Electronic supplementary information (ESI) available. See DOI: 10.1039/c4dt00393d

Cobalt ferrite nanoparticles ($CoFe_2O_4$ MNPs) are among the magnetic nano-particles that have been proposed for several bioapplications[9] such as contrast enhancement candidates in magnetic resonance imaging (MRI), hyperthermia agents, magnetically tagging devices of bioentities and drug carriers.[10] Although wet chemistry preparation methods in organic solvents are highly efficient in controlling the main features of magnetic nanoparticles like the size, shape, crystallinity and monodispersity, the hydrophobic nature of the derived MNPs impediments their direct use in bioapplications and further functionalization is needed.[11]

Since hydrophilicity is essential for *in vitro* and *in vivo* applications, phase transfer becomes necessary. In general, several strategies exist and are applied for phase transfer:[12] (a) ligand exchange where a hydrophobic ligand is replaced by a hydrophilic one, (b) ligand modification with a variety of bioactive molecules, (c) additional coating layers through hydrophobic interactions with the original ligand, (d) silanization and (e) polymer coating, where hydrophobic MNPs are encapsulated into the hydrophobic domains of the supramolecular structures formed by amphiphilic molecules through hydrophobic interactions and van der Waals forces. The concept of using amphiphilic block copolymers for the stabilization of hydrophobic MNPs in water has been widely exploited.[13] In contrast, the literature on the use of HMWSPs to stabilize hydrophobic MNPs in aqueous media is relatively poor.[14] Nevertheless, such applications of HMWSPs are of particular interest, since they are much easier to be synthesized than block copolymers, using a one-step synthetic procedure (free radical polymerization of adequate monomers or chemical modification of the backbone).

In the present study, the possibility of using micelle-like structures formed by HMWSPs to stabilize hydrophobic $CoFe_2O_4$@OAm MNPs in aqueous media was evaluated. Thus, a series of HMWSPs consisting of a poly(sodium methacrylate) backbone (PMANa) and dodecyl-pendent chains were prepared through free radical copolymerization of methacrylic acid (MAA) and dodecylmethacrylate (DMA). The synthetic conditions were adjusted, in order to vary the dodecyl-content and the molecular weight of the samples. Moreover, a sample of a comparable hydrophobic content was prepared through grafting of dodecyl chains onto a poly(sodium acrylate) backbone (PANa), in an attempt to investigate the possible influence of the synthetic protocol (copolymerization or "grafting-to" methodology). The synthesis and characterization of the HMWSP used and the hydrophobically modified $CoFe_2O_4$@OAm MNPs is first discussed in the present work. The major part of the work is devoted to the investigation of the ability of these HMWSPs to disperse the hydrophobically modified $CoFe_2O_4$@OAm MNPs in water ($CoFe_2O_4$@HMWSP), in conjunction with the self-organization properties of the polymers in an aqueous environment. Moreover, NMR relaxivity studies of aqueous suspensions of $CoFe_2O_4$@HMWSP were performed and compared with the hydrophilically modified $CoFe_2O_4$@OAm MNPs, resulted from (i) an additional coating layer with the positively charged molecule of cetyltrimethyl ammonium bromide ($CoFe_2O_4$@CTAB) and (ii) ligand exchange with 2,3-dimercaptosuccinic acid ($CoFe_2O_4$@DMSA).

Experimental part

Materials

The monomer methacrylic acid (MAA), the fluorescent probe Nile Red, dodecylamine (DAm) as well as iron(III) acetylacetonate (≥97.0%, $Fe(acac)_3$) were purchased from Fluka, while the monomer dodecyl methacrylate (DMA) was obtained from Acros. The homopolymer poly(acrylic acid) (PAA) with a molecular weight of 5000 g mol^{-1}, the initiator azobisisobutyronitrile (AIBN), the coupling agent *N*,*N*′-dicyclohexylcarbodiimide (DCC), cobalt(III) acetylacetonate (≥99.9%, $Co(acac)_3$), oleylamine (OAm) and the solvents *N*,*N*-dimethylformamide (DMF), tetrahydrofuran (THF), dimethyl sulfoxide (DMSO), chloroform, ethanol, methanol, petroleum ether, deuterated dimethyl sulfoxide (d_6-DMSO) and deuterated water (D_2O) were all purchased from Aldrich. *meso*-2,3-Dimercaptosuccinic acid (DMSA) was purchased from Tokyo Chemical Industry (TCI) Co. Ltd and cetyltrimethyl ammonium bromide (CTAB) (98.0%) was purchased from Alfa Aesar. Ultrapure 3D-water was obtained by means of SG Waters apparatus.

Synthesis of amphiphilic copolymers and $CoFe_2O_4$@OAm nanoparticles

Synthesis of the P(MANa-co-DMA) copolymers. Typically, a THF solution of MAA, DMA and AIBN was added in a round-bottom flask equipped with a reflux condenser. The mixture was degassed with Ar for 2 hours and the reaction was performed by heating at 70 °C and left overnight under stirring. The polymers were recovered through precipitation in petroleum ether and dried under vacuum at 40 °C. The acid form of the copolymer, P(MAA-co-DMA), was transformed into the sodium salt form, P(MANa-co-DMA), through dissolution in an aqueous NaOH solution. The copolymer was purified through dialysis and recovered through freeze-drying.

Synthesis of the P(ANa-co-DAAm) copolymer. Briefly, in a three-necked flask equipped with a reflux condenser appropriate amounts of PAA (M_W = 5000 g mol^{-1}) and DAm were first dissolved in DMF at 60 °C. Then, DCC dissolved in a small amount of DMF was added dropwise to the solution and the mixture was left under stirring at 60 °C. After 24 h, the solution was cooled at room temperature; vacuum filtered to remove the unwanted dicyclohexyl urea byproduct and the required volume of a 1 M NaOH aqueous solution was added to the copolymer solution. The sodium salt form of the precipitated copolymer was washed several times with DMF and then with methanol in order to remove unreacted segments and byproducts. The final polymer was filtered under vacuum and dried in a vacuum oven at 60 °C.

Solvothermal synthesis of $CoFe_2O_4$@OAm nanoparticles. Based on our previous results[15] $CoFe_2O_4$@OAm MNPs have been prepared solvothermally by dissolving 1.8 mmol $Fe(acac)_3$ and 0.9 mmol $Co(acac)_3$ in 12 mL of OAm. The resulting solu-

tion was stirred thoroughly and then transferred into a 23 mL Teflon-lined stainless-steel autoclave. The autoclave was placed in an electrical oven and the temperature was raised up to 200 °C (4 °C min^{-1}) for 24 h. Then the autoclave was cooled to room temperature with a steady rate of 5 °C min^{-1} and the product was washed with ethanol. The washing process *via* centrifugation cycles (10 000 rpm) was repeated at least three times, and the excess of OAm and unreacted precursors was removed by discarding the supernatant. Finally, $CoFe_2O_4$@OAm MNPs were obtained as a black-brown precipitate.

Stabilization of hydrophobic $CoFe_2O_4$@OAm MNPs in water

Preparation of aqueous $CoFe_2O_4$@HMWSP dispersions. The hybrid $CoFe_2O_4$@HMWSP materials were prepared using a solvent mixing methodology. Briefly, an appropriate amount of HMWSP was dissolved in 3D water and left under stirring overnight. A small volume of a THF dispersion of $CoFe_2O_4$@OAm MNPs was added to the aqueous polymer solution. The polymer/MNPs mixing ratio was adjusted to 10/1 by weight and sonicated in a Branson 1510 70 W, 40 kHz sonicator. No precipitation was observed upon mixing the polymer solution with the $CoFe_2O_4$@OAm dispersion. The mixture was left at 40 °C until full evaporation of THF. At this stage, precipitation of a fraction of MNPs was eventually observed. This fraction was discarded and the supernatant was used for further studies.

Preparation of aqueous $CoFe_2O_4$@CTAB dispersions. The as-prepared hydrophobic $CoFe_2O_4$@OAm MNPs were converted to hydrophilic ones *via* the cationic surfactant CTAB ($CoFe_2O_4$@CTAB) following a previously reported method.[16] An aqueous solution of CTAB (0.02 M) and a suspension of $CoFe_2O_4$@OAm MNPs (3 mg) in chloroform (0.5 mL) were prepared and mixed to result in an oil-in-water microemulsion. The resulting mixture was sonicated for more than 5 h until the chloroform was completely evaporated, leaving a brownish aqueous solution denoted as $CoFe_2O_4$@CTAB MNPs.

Preparation of aqueous $CoFe_2O_4$@DMSA dispersions. A ligand exchange method was followed where the hydrophobic surface of $CoFe_2O_4$ MNPs was modified to hydrophilic one. A mixture of the capping agent DMSA (10 mg) in DMSO (0.5 mL) was added to a mixture of $CoFe_2O_4$@OAm MNPs (10 mg) in toluene (3 mL).[17] The resulting mixture was sonicated for 15 min and stirred for 24 h at room temperature. The supernatant was discarded and the resulting $CoFe_2O_4$@DMSA MNPs were successfully mixed and centrifuged with ethanol several times to remove free OAm molecules before being dispersed in water. The pH of the aqueous suspension increased up to 10 with 1 M NaOH solution in order to deprotonate the carboxylic groups and thiol groups (p*K* 9.2) of the DMSA[17] and then adjusted to 5 with 1 M HNO_3 solution in order to achieve better dispersion of the $CoFe_2O_4$@OAm MNPs.[17,18] The resulting suspension is stable in water for a prolonged period of time and denoted as $CoFe_2O_4$@DMSA MNPs.

Characterization techniques

^{1}H-NMR spectra of the copolymers in d_6-DMSO or D_2O were obtained on a Bruker Avance DPX 400 MHz spectrometer. The acid form of the copolymers, soluble in THF, was used for gel permeation chromatography (GPC) characterization. Two PLgel MiniMix columns "C" and "D" (molecular range 4000–340 000 g mol^{-1}) were used and calibrated with polystyrene standards. THF was used as an eluent. The elution rate was 0.5 mL min^{-1}. The powder X-ray diffraction (XRD) diagram was obtained using a 2-cycle Rigaku Ultima + diffractometer (40 kV, 30 mA, CuKα radiation) with Bragg–Brentano geometry (detection limit 2% approximately). The size was estimated by taking the full width at half-maximum (FWHM) of the most intense peak (311) and based on the Debye–Scherrer equation.[19] Magnetic measurements were performed on a 1.2H/CF/HT Oxford Instruments VSM at 300 K as a function of the applied field (1 T) and on a superconducting quantum interference device (Quantum Design MPMS-5 SQUID). Elemental analysis was performed by inductively coupled plasma optical emission spectroscopy (ICP-OES, ICP Simultané VARIAN Vista Axial).

Physicochemical characterization

Nile Red fluorescence probing. Steady-state fluorescence spectra of Nile Red were recorded on a Perkin Elmer LS50B luminescence spectrometer. A small volume (5 μL) of a stock THF solution, containing 1×10^{-3} M Nile Red, was added to 3 mL of the aqueous polymer solution. The final concentration of the probe was, thus, fixed at 1.7×10^{-6} M. The maximum intensity of the emission peak of Nile Red in the region 600–650 nm, after excitation at 550 nm, was used to detect the formation of hydrophobic microdomains. The excitation and emission slits were fixed at 10 nm.

Dynamic light scattering and electrophoresis measurements. ζ-Potentials were determined by electrophoretic measurements, carried out at 25 °C by means of the NanoZetasizer, Nano ZS Malvern apparatus. The incident light source was a 4 mW He–Ne laser at 633 nm and the intensity of the scattered light was measured at 173°. The mean hydrodynamic diameter was determined from the obtained apparent diffusion coefficient through the Stokes–Einstein equation.

Transmission electron microscopy. TEM experiments were carried out using a JEM 2100 microscope operating at 200 kV. For the TEM investigation of pure NMPs, diluted THF dispersions were used, whereas aqueous solutions/dispersions were used for the TEM investigation of pure polymers or MNP/HMWSP hybrids. A drop of the solution/dispersion at the desired polymer concentration was deposited onto a carbon coated grid and allowed to evaporate at room temperature.

Zero-field-cooling/field-cooling (ZFC/FC). ZFC/FC measurements were performed on a superconducting quantum interference device (Quantum Design MPMS-5 SQUID); the sample was cooled from room temperature to 5 K without applying a magnetic field and then was heated back to room temperature under a magnetic field of 50 Oe, and the blocking temperature value (T_b) was obtained. The effective anisotropy constant (K_{eff}) was calculated according to the equation:[20] $25 \times k_B \times T_b = K_{eff} \times V$, where k_B is the Boltzmann constant, T_b is the blocking temperature and V is the particle volume.

NMR transverse relaxation time (T_2). T_2 measurements were performed on a 500-MR NMR Spectrometer (500 MHz, Agilent Technologies) at 25 °C, using a Carr-Purcell-Meiboom-Gill (CPMG) pulse sequence. The metal ion concentration (Fe + Co) of aqueous solutions was measured by inductively coupled plasma optical emission spectroscopy (ICP-OES). T_2 was measured for a range of concentrations (0.05–0.8 mM) of metal ions of the aqueous suspensions of $CoFe_2O_4$@P(ANa-co-DMAAm), $CoFe_2O_4$@CTAB and $CoFe_2O_4$@DMSA.

Results and discussion

Synthesis and characterization of the copolymers

A series of HMWSPs were evaluated in terms of their ability to stabilize hydrophobically modified $CoFe_2O_4$ MNPs in water. These polymers, P(MANa-co-DMA), are based on a carboxylate backbone and dodecyl-side chains. As shown in Scheme 1a, they have been prepared through free radical copolymerization (FRP) of MAA and DMA, followed by neutralization of the polyacid. Three P(MANa-co-DMA) copolymers differing in the composition or molecular weight were successfully prepared by the variation of the monomer feed ratio and the initiator/monomer ratio. Alternatively, a "grafting-to" methodology was applied to prepare an additional HMWSP, namely P(ANa-co-DAAm), through the coupling reaction of the carboxylic groups of PAA and the amine group of DAm using DCC as a condensing agent, followed by neutralization of the product (Scheme 1b). A low molecular weight PAA homopolymer was used to synthesize the latter product.

The copolymers were characterized by ^{1}H-NMR and GPC as far as their chemical composition and molecular weight are concerned. For the characterization of the P(MANa-co-DMA), we took advantage of the solubility of the acid form of these polymers P(MAA-co-DMA) in organic solvents. The ^{1}H-NMR spectra of the amphiphilic P(MAA-co-DMA) copolymers in d_6-DMSO are shown in Fig. 1. The peaks in the region 1.3–2.2 ppm are attributed to the methyl- and methylene groups of the main polymer chain. The strong signal at ~1.3 ppm corresponds to the aliphatic groups of DMA while the signal at 0.8–0.9 ppm is attributed to the characteristic peak of the $-CH_3$ groups of both MAA and DMA. The same peaks are also observed in the ^{1}H-NMR spectrum of P(ANa-co-DAAm) in D_2O, since its chemical structure is similar to that of P(MAA-co-DMA) copolymers. The major difference is that the peak at 0.8–0.9 ppm is now much sharper, as a consequence of the absence of the methyl group in the structure of sodium acrylate. The DMA content of the P(MAA-co-DMA) copolymers and the DAAm content of the P(ANa-co-DAAm) copolymer were determined from the integration ratio of the peaks at 0.8–0.9 ppm and 1.3 ppm. The results are shown in Table 1. As can be seen, P(MANa-co-DMA) copolymers with hydrophobic contents of ~25% (mol mol^{-1}) and 12% (mol mol^{-1}) have been obtained. Moreover, the composition of the latter copolymer is close to that of the P(ANa-co-DMAAm) copolymer, derived through the "grafting-to" methodology.

GPC characterization of P(MAA-co-DMA) copolymers was performed in THF (Fig. S1†). The number-average molecular weight (M_n) and the weight-average molecular weight (M_w) are tabulated in Table 1. As expected for FRP reactions, unimodal GPC curves with quite broad molecular weight distributions (M_w/M_n ~ 2–2.5) are observed for all three copolymers. More-

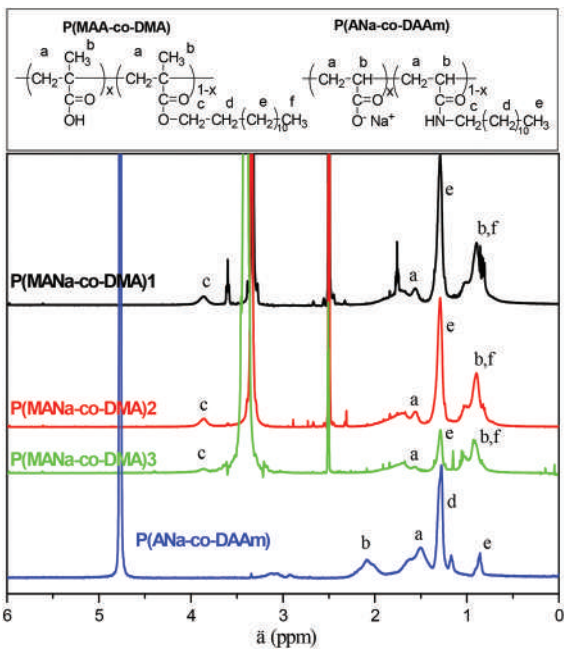

Fig. 1 ^{1}H-NMR spectra of the P(MAA-co-DMA) copolymers in d_6-DMSO and the copolymer P(ANa-co-DAAm) in D_2O.

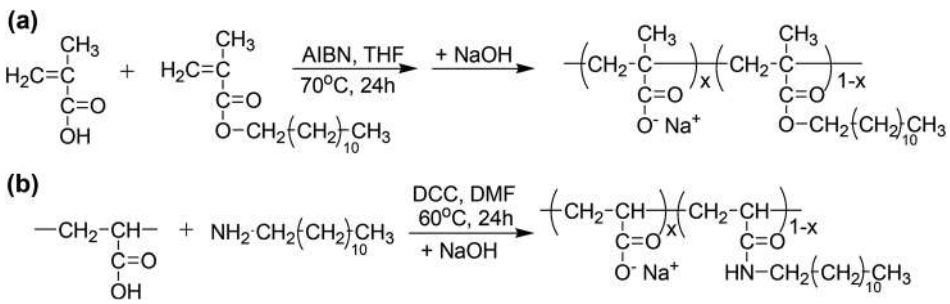

Scheme 1 Synthesis of HMWSP: (a) P(MANa-co-DMA) and (b) P(ANa-co-DAAm) through FRP and "grafting-to" methodology, respectively.

Table 1 Physicochemical characterization results of the amphiphilic copolymers used in the present work

Copolymer	Initiator/monomer molar ratio	Composition (^{1}H-NMR)[a]	M_n (g mol^{-1}) (GPC)	M_w (g mol^{-1}) (GPC)	ζ-potential (mV)	CMC[c] (wt%)
P(MANa-co-DMA)1	0.005	75	27 800	73 600	−40.7	0.002
P(MANa-co-DMA)2	0.015	77	10 000	24 600	−52.1	0.002
P(MANa-co-DMA)3	0.015	88	6400	13 800	−49.7	0.2
P(ANa-co-DAAm)	—	90	—	7500[b]	−46.8	0.1

[a] % moles of MANa or ANa units. [b] Calculated from the nominal mass of PAA and the composition of the copolymer, as found through ^{1}H-NMR. [c] From Nile Red probing.

over, through the adequate variation of the monomer/initiator molar ratio, copolymers with M_w ranging from ~14 000 up to 74 000 g mol^{-1} are obtained. It was not possible to perform the GPC characterization of P(ANa-co-DAAm) in THF, due to its insolubility in organic solvents. Our attempts to perform the same characterization using an aqueous eluent were unsuccessful, probably due to the amphiphilic character of the copolymer in water. Nevertheless, we were able to calculate the molecular weight of the copolymer using the nominal mass of the precursor PAA and the chemical composition of the product, as determined through the ^{1}H-NMR characterization. As shown in Table 1, this copolymer is comparable to the P(MANa-co-DMA)3 sample, as it concerns both the hydrophobic content and the molecular weight.

Synthesis and characterization of the oleylamine coated $CoFe_2O_4$ nanoparticles

Bragg reflections in the 2θ range of 10–90° confirm the formation of cobalt ferrite (PDF card no. 22-1086). The characteristic peaks of the cubic spinel structure *Fd3m* (227) are evident in Fig. 2a; the lattice parameter was calculated, 8.401(0) Å, and found to be close to the bulk value (a = 8.392(1) Å) indicating the high crystallinity of the particles. The average crystalline size of 9.4(1) nm was estimated by the Debye–Scherrer equation. Saturation magnetization (M_s) of the MNPs was measured on a VSM (Fig. 2b). The normalized M_s was 85 emu g^{-1} which is close to the bulk[21] and the coercive field was 283 Oe. This value is among the highest for small sized $CoFe_2O_4$ MNPs when compared to results reported in the literature as for 12 nm M_s = 50.00 emu g^{-1} (value corrected by TGA data),[17] for 10 nm M_s = 60.59 emu g^{-1} (net magnetization value)[22] and for 8 nm M_s = 65.30 emu g^{-1} (net magnetization value).[23] The magnetization enhancement can be attributed to oxygen vacancies in the spinel that reduce the dead layer (spin disorder layer structure),[24] meanwhile reduction of the dead layer may be achieved through the coordination of σ-donors such as oleylamine, on the metal core since they can increase the spin–orbit coupling due to a decrease of the crystal field splitting which favors the uplift of the magnetocrystalline anisotropy of the surface layer.[25] Fig. 2c shows a TEM image of

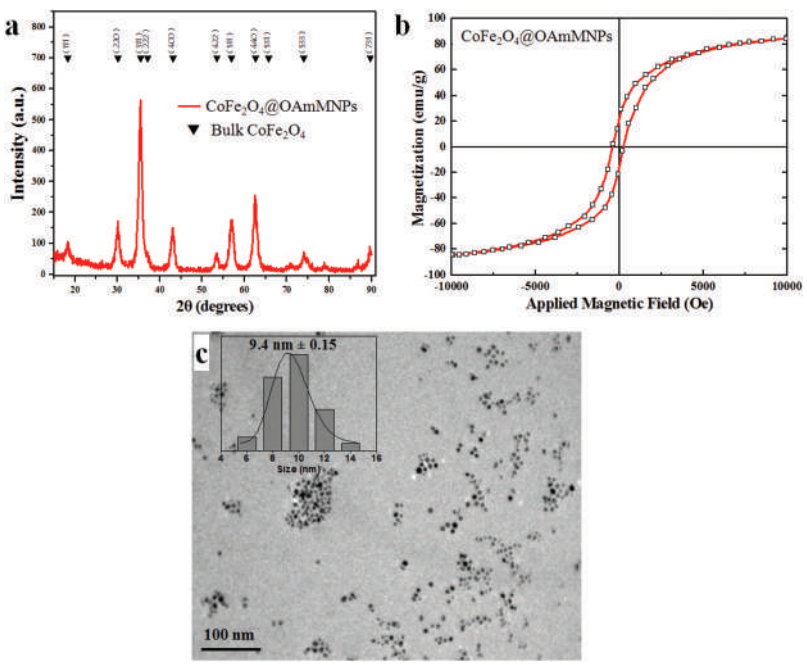

Fig. 2 (a) X-Ray diffraction pattern of the as-prepared $CoFe_2O_4$@OAm MNPs, (b) VSM measurements and (c) TEM micrographs of $CoFe_2O_4$@OAm MNPs (scale bar: 100 nm).

oleylamine-coated $CoFe_2O_4$@OAm MNPs dispersed in THF. The nanoparticles are almost spherical with a relatively uniform size of 9.0 ± 0.15 nm (σ = 1.5%) and narrow size distribution. In addition ZFC/FC measurements showed that the sample is in a ferrimagnetic state below T_b (T_b = 300 K) (Fig. S2†); K_{eff} was calculated as 29.7 kJ m^{-3}. Consequently, the resulting MNPs exhibit enhanced M_s, high anisotropy constant, relatively small size, high crystallinity and narrow size distribution characteristics that are essential for further applications.[26]

The use of HMWSPs to transfer the hydrophobic $CoFe_2O_4$@OAm MNPs in water

Self-assembly of the amphiphilic copolymers in aqueous media. Before investigating the possibility of transferring the hydrophobic $CoFe_2O_4$@OAm MNPs in water with the help of the HMWSPs used in the present study, the knowledge of the potential self-organization (eventually forming micelle-like supramolecular structures) of the polymers in water is a prerequisite. Thus, we first determined the critical micelle concentrations (CMC) of the copolymers in aqueous solution by fluorescence probing using Nile Red as a fluorescence probe. It is well known that this probe is poorly soluble in water but its solubility increases in a less polar environment. Moreover, the probe is almost non-fluorescent in water and other polar solvents, whereas it is strongly fluorescent in less polar environments, showing an intense emission peak in the region 600–650 nm.

The maximum fluorescence intensity of the emission peak of Nile Red at 600–650 nm is plotted in Fig. 3a as a function of the concentration of the polymer. As can be seen, at low polymer concentrations, the maximum intensity of Nile Red is low, indicating that the probe detects a purely hydrophilic environment. However when the polymer concentration increases above the critical value (CMC), the intensity increases sharply. Obviously, the amphiphilic copolymers are now self-organized into micellar-like structures, where the pendant alkyl chains form the hydrophobic core and the anionic polyelectrolyte backbones form the hydrophilic corona, thus stabilizing the system in water. As a consequence, the probe is now solubilized in the hydrophobic region of the formed polymeric micellar structures and "senses" a hydrophobic microenvironment. The CMC values of the amphiphilic copolymers are tabulated in Table 1. These values are low, since the hydrophobic content of the copolymers is rather high. Moreover, it is evident that CMC decreases drastically from ~0.1% (wt/v) to ~0.002% (wt/v) as the hydrophobic content of the copolymers increases from ~12% (mol mol^{-1}) to ~25% (mol mol^{-1}). Finally, it is clear that the crucial factor controlling CMC is the hydrophobic content and not the molecular weight (compare P(MANa-co-DMA)1 and P(MANa-co-DMA)2) or the exact chemical structure of the copolymer (compare P(MANa-co-DMA)3 and P(ANa-co-DAAm)). Moreover, since CMC depends on the chemical structure of the HMWSPs, the polymer concentration level is expected to be critical for the encapsulation (and consequently the amount of MNPs, magnetization, *etc.*) of $CoFe_2O_4$@OAm MNPs. For example, at a concentration C = 0.005 wt%, the copolymers P(MANa-co-DMA)3 and P(ANa-co-DAAm) are not expected to exhibit any encapsulation ability (C < CMC), while the copolymers P(MANa-co-DMA)1 and P(MANa-co-DMA)2 are expected to encapsulate the hydrophobic MNPs (C > CMC).

The size distribution and the charge of these supramolecular assemblies at concentrations above CMC were characterized by DLS and ζ-potential measurements, respectively. As can be seen, in Table 1, strongly negative ζ-potential values are measured for all copolymers, as a consequence of the anionic nature of the polyelectrolytes used. Such values are typical of micelles of amphiphilic diblock copolymers, consisting of a hydrophobic and an anionic PMANa block.[27]

The size distribution of the copolymers above CMC is shown in Fig. 3b. It is evident that several relaxation modes are present. In this representation of the DLS results, the slowest relaxation mode is identified by large sizes of the order of a few hundred nanometers. This slow mode is often observed in polyelectrolyte solutions at low ionic strength and

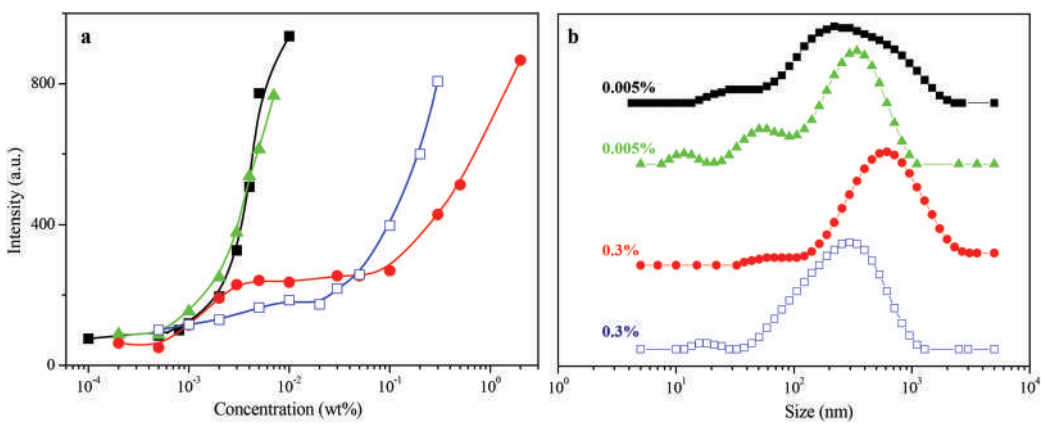

Fig. 3 (a) Dependence of the maximum fluorescence intensity of the emission of Nile Red at 600–650 nm on the polymer concentration and (b) distribution of the hydrodynamic diameter, as determined by DLS for (■) P(MANa-co-DMA)1, (▲) P(MANa-co-DMA)2, (●) P(MANa-co-DMA)3 and (□) P(ANa-co-DAAm). The polymer concentrations for the DLS study, shown in the figure, are above CMC.

it could be attributed to diffusive relaxation of cooperative multichain fluctuations or domains.[28] However, in the case of amphiphilic diblock copolymers it could also correspond to large sized objects like large compound micelles.[29] Moreover, for all copolymers, an intermediate relaxation mode is also present, identified either as a shoulder or a clear population with a mean size of the order of a few tens of nanometers, corresponding to the polymeric micelles. Finally, in most cases, a fast relaxation mode is also present, corresponding to an average diameter of ~10–20 nm. This mode probably is that of single copolymer chains or unimolecular micelles.

In order to gain more inside information on the supramolecular structures formed by the copolymers in aqueous solution, we proceeded to TEM characterization at concentrations below and above CMC. Some representative results concerning P(MANa-co-DMA)1 are shown in Fig. 4. Below the CMC the copolymer is molecularly dissolved in water and thus no special structures could be detected (Fig. 4a). Above CMC, the copolymer forms spherical structures, either micelles with a size of the order of ~30–40 nm (Fig. 4b) or large compound micelles with sizes corresponding to the slow relaxation mode observed by DLS (insets of Fig. 4b). A rather similar behavior was also observed for P(MANa-co-DMA)2. On the other hand, no isolated structures could be observed for P(MANa-co-DMA)3 and P(ANa-co-DAAm). This, apparently, is a consequence of the higher concentration used for the study, since the CMC values of the latter copolymers are much higher. Finally, it should be noted that both TEM and DLS techniques showed that the supramolecular structures formed are quite polydisperse in size. This polydispersity is probably a consequence of the broad molecular weight distribution and the random architecture of our HMWSPs.

Study of the $CoFe_2O_4$@HMWSP nanohybrids. To transfer the hydrophobic $CoFe_2O_4$@OAm MNPs in water with the help of the aforementioned HMWSPs, a solvent mixing protocol was applied. THF was chosen as the organic solvent, because it is miscible with water and at the same time it is a good dispersant of the MNPs. In fact, when we applied this protocol using our HMWSPs at a concentration below CMC, the hydrophobic $CoFe_2O_4$@OAm MNPs could not be dispersed in water and macroscopic phase separation was observed. On the other hand, as exemplified in Scheme 2, above CMC, the major part of the hydrophobic $CoFe_2O_4$@OAm MNPs (in the mixing ratio used) was able to enter into the hydrophobic cores of the micellar polymeric structures and MNPs were effectively stabilized in water. This was evidenced by the stable brownish coloration of the aqueous mixture (a representative photo at a high $CoFe_2O_4$@HMWSP concentration, corresponding to that of the NMR relaxivity measurements, is shown in Scheme 2).

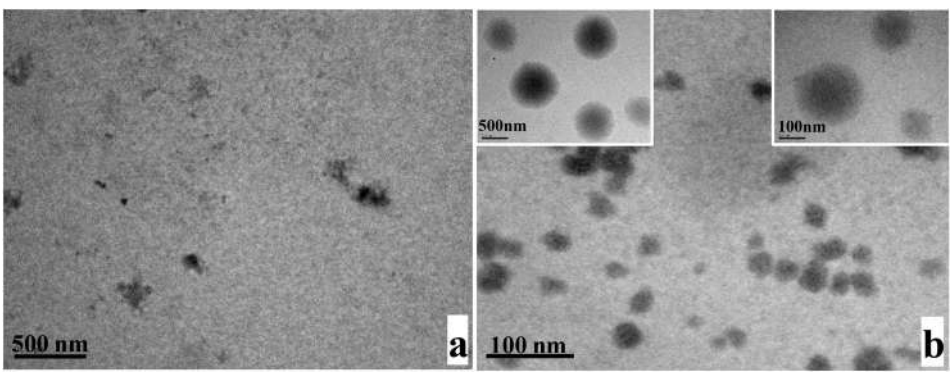

Fig. 4 TEM images of (a) 0.001 wt% (below CMC, scale bar: 500 nm) and (b) 0.005 wt% (above CMC, scale bar: 100 nm) aqueous P(MANa-co-DMA)1 solutions. The scale bars in the insets are 500 nm (left) and 100 nm (right).

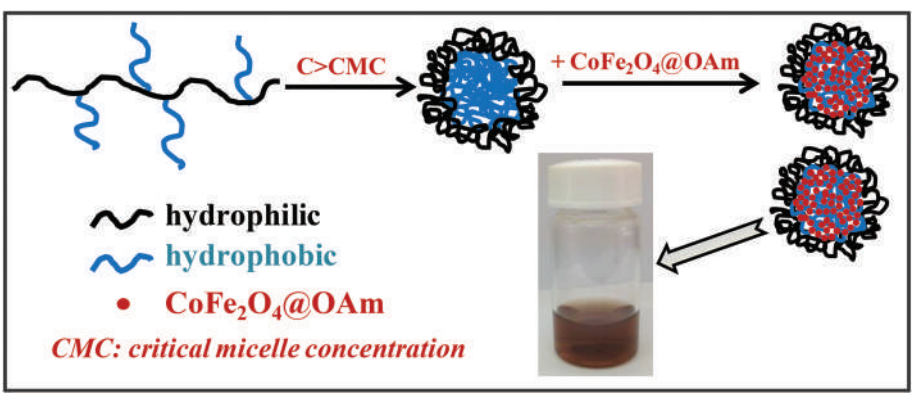

Scheme 2 Schematic depiction of the stabilization of $CoFe_2O_4$@HMWSP nanohybrids in water.

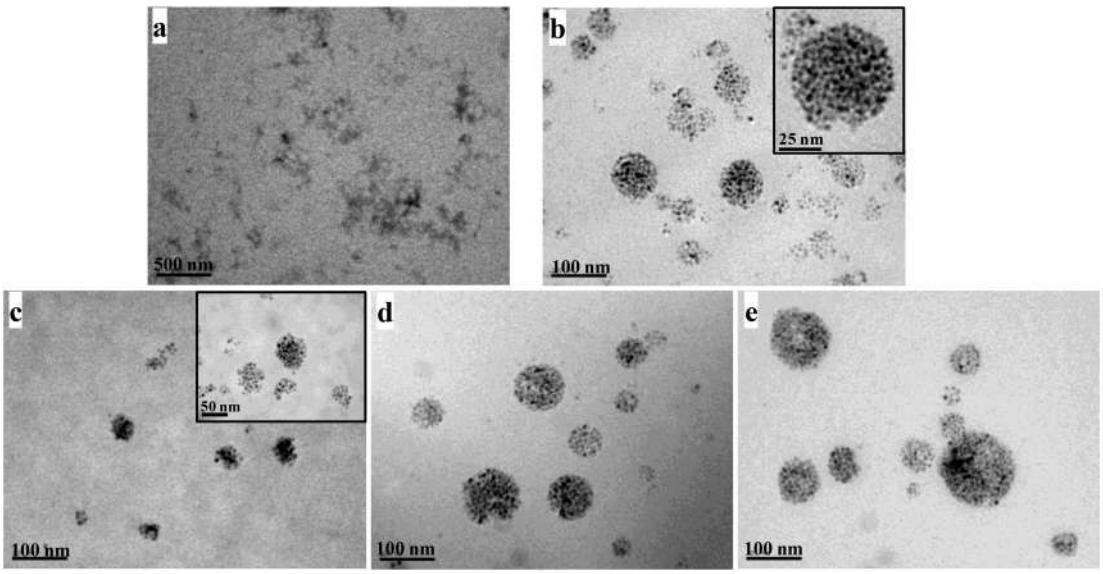

Fig. 5 TEM images of $CoFe_2O_4$@P(MANa-co-DMA)1 (a) below CMC (0.001 wt%, scale bar: 500 nm) and (b) above CMC (0.005 wt%); (c) $CoFe_2O_4$@P(MANa-co-DMA)2 above CMC (0.005 wt%), (d) $CoFe_2O_4$@P(MANa-co-DMA)3 above CMC (0.3 wt%) and (e) $CoFe_2O_4$@P(ANa-co-DAAm) above CMC (0.3 wt%). The scale bars of b–e are 100 nm, while the scale bars of insets in b and c are 25 nm and 50 nm, respectively.

Representative TEM images of the hydrophobic $CoFe_2O_4$@P(MANa-co-DMA)1 mixtures below and above CMC, using this protocol, are shown in Fig. 5a and 5b, respectively. Below CMC, no micelles are formed and no MNPs could be detected on the TEM grid. In agreement with the discussion in Fig. 3a, when the copolymer is molecularly dissolved in water, the polymeric chains are not capable of dispersing the hydrophobic magnetic nanoparticles in aqueous solution (Fig. 5a). On the other hand, at a polymer concentration higher than CMC, one can observe the effective encapsulation of the magnetic nanoparticles into the formed polymer micelle-like structures (Fig. 5b). The hydrophobic $CoFe_2O_4$@OAm MNPs are located in the hydrophobic core of the micelles formed by P(MANa-co-DMA)1, while the hydrophilic MANa groups maintain the whole system stable in water. A similar behavior is also exhibited by the hydrophobic $CoFe_2O_4$@P(MANa-co-DMA)2 as well (Fig. 5c). In the TEM images, as a consequence of the high contrast of the MNPs, the hydrophilic part of the micelles cannot be seen but only the hydrophobic cores with the incorporated $CoFe_2O_4$@OAm MNPs are observable. In fact, for this reason, we were also able to observe the nanohybrid structures formed upon mixing the hydrophobic $CoFe_2O_4$@OAm MNPs with P(MANa-co-DMA)3 (Fig. 5d) and P(ANa-co-DAAm) (Fig. 5e), although a rather high polymer concentration is used in order to ensure the micellization of the copolymers. It is noteworthy that the size distribution of the cores of the $CoFe_2O_4$@HMWSP nanohybrids is large. Thus, in a rather good qualitative agreement with the DLS findings in Fig. 3b, $CoFe_2O_4$-loaded cores of large sizes (more than 100 nm), corresponding to large-compound micelles, as well as of smaller sizes (a few tens of nanometers), corresponding to polymeric micelles, are observable for most nanohybrids. In fact, it is interesting to note that assemblies of nanohybrids corresponding to polymeric micelles are mainly observed in the case of the P(MANa-co-DMA)2 copolymer. This is in line with the DLS findings, where the population of polymeric micelles is more pronounced, as compared to the other copolymers.

NMR relaxation measurements

The characteristics of the as-prepared $CoFe_2O_4$@OAm MNPs (D = 9.4 nm, M_s = 85 emu g^{-1}, K_{eff} = 29.7 kJ m^{-3}) made them challenging candidates for potential bioapplications including in magnetic resonance imaging (MRI) as they exhibited enhanced M_s, small size, narrow size distribution and K_{eff} values that are among the proposed optimum values which are $10 < D < 30$ nm, $60 < M_s < 100$ emu g^{-1} and $5 < K_{eff} < 40$ KJ m^{-3}.[30] The efficiency of the MNPs to act as T_2 contrast agents for MRI depends on the relaxation process of protons when placed in an external magnetic field, namely the transverse or spin–spin relaxation process (T_2) while they have a much smaller effect on the longitudinal or spin–lattice relaxation process (T_1). The transverse T_2 relaxation time of hydrogen protons of pure water at various concentrations of the samples was determined using an NMR spectrometer. Moreover, the efficiency of the MNPs to act as T_2 contrast agents is determined in terms of the transverse relaxivity (r_2) according to eqn (1).[31] For comparison purposes, three different methodologies were applied to convert the as-prepared hydrophobic $CoFe_2O_4$@OAm MNPs into hydrophilic and the transverse relaxivity (r_2) of each system at various concentrations has been determined: (i) addition of a coating layer (CTAB), (ii) the ligand exchange procedure (DMSA) and (iii) polymer encapsulation (P(ANa-co-DAAm)).

$$R_2 = \frac{1}{T_2} = \frac{1}{T_2{}^0} + r_2 C \quad (1)$$

where T_2 is the observed proton relaxation time in the presence of MNPs, $T_2{}^0$ is the proton relaxation time of pure water and C is the concentration of the contrast agent. T_2 was measured for a range of concentrations (0.05–0.8 mM) of metal ions of the aqueous suspensions of $CoFe_2O_4$@P(ANa-co-DMAAm), $CoFe_2O_4$@CTAB and $CoFe_2O_4$@DMSA. All measurements showed perfect monoexponential decay, which is characteristic of magnetic compounds that enhance the water proton relaxivity by diffusion. Indeed, a linear concentration dependence of R_2 is experimentally observed (Fig. 6), permitting the determination of r_2 for the resulting hydrophilic MNPs obtained through the three surface modification procedures. In addition, the ζ-potential of these hydrophilic MNPs was determined as an indicator of the good colloidal stability of the aqueous suspensions.[32] ζ-potential and r_2 values are summarized in Table 2. $CoFe_2O_4$@P(ANa-co-DAAm) was selected among the $CoFe_2O_4$@HMWSP nanohybrids since it bears a comparable surface charge (absolute value) to $CoFe_2O_4$@CTAB. The negative charge of $CoFe_2O_4$@DMSA and $CoFe_2O_4$@P(ANa-co-DAAm) MNPs is attributed to the $-COO^-$ groups, while the positive charge of $CoFe_2O_4$@CTAB MNPs is due to the $-N^+(CH_3)_3$ functional group.

The r_2 relaxivity value of $CoFe_2O_4$@P(ANa-co-DAAm) is lower than that of $CoFe_2O_4$@CTAB while it is ~4 times higher than that of $CoFe_2O_4$@DMSA. This difference is attributed to the structure and size of each coating agent. The metal core of $CoFe_2O_4$@P(ANa-co-DAAm) is effectively isolated from the exterior water molecules since it is confined within the hydrophobic polymer core (Fig. 5e).[33] The dramatic decrease of the r_2 value in the case of $CoFe_2O_4$@DMSA is associated with the lower colloidal stability and the formation of a shell-like extended coating. DMSA would be expected to increase r_2 values, since it is a small ligand with carboxylic groups. However, an opposite effect on the r_2 relaxivity is observed. The anchored carboxyl groups (COO^-) formed a shell-like stable coating, later on reinforced by the disulfide (S–S) cross-linking between different DMSA molecules.[34] The presence of free carboxylic groups as well as the absence of –SH groups have been confirmed by the FT-IR spectra (Fig. S3†). An analogous behavior was observed previously by us for $NiFe_2O_4$ nanoparticles modified with CTAB and DMSA.[35]

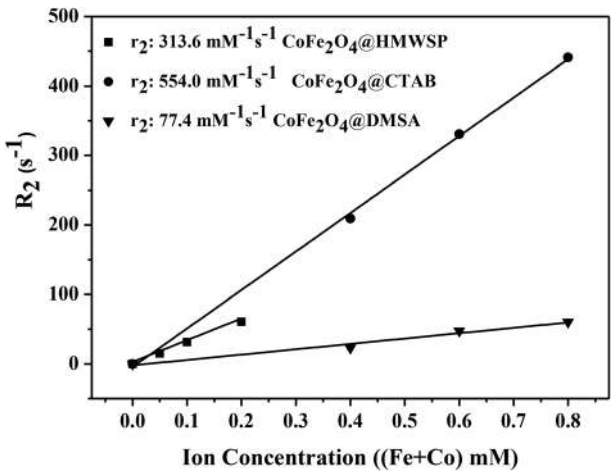

Fig. 6 Transverse relaxation measurements of aqueous suspensions of $CoFe_2O_4$@P(ANa-co-DAAm) (■), $CoFe_2O_4$@CTAB (●) and $CoFe_2O_4$@DMSA (▼).

Table 2 ζ-potential and r_2 relaxivity values of $CoFe_2O_4$ MNPs with different coatings in water

Sample	Surface coating	ζ-potential (mV)	r_2 (mM^{-1} s^{-1})
$CoFe_2O_4$@CTAB	CTAB	+34.4	554.0
$CoFe_2O_4$@P(ANa-co-DAAm)	P(ANa-co-DAAm)	−38.0	313.8
$CoFe_2O_4$@DMSA	DMSA	−19.8	77.4

However, $CoFe_2O_4$@CTAB and $CoFe_2O_4$@P(ANa-co-DAAm) formed better aqueous colloidal dispersions than $CoFe_2O_4$@DMSA. Nevertheless, all samples affected the relaxivity in a positive way and afforded r_2 values comparable to and even higher than those previously reported for $CoFe_2O_4$ MNPs at similar sizes. For $CoFe_2O_4$ MNPs of 8 nm following a similar ligand exchange procedure where oleic acid and oleylamine are exchanged with DMSA, the r_2 value was found to be 392.4 mM^{-1} s^{-1} (T_2 values recorded at 9.4 T),[23] while for spherical $CoFe_2O_4$ MNPs with sizes 6 nm, 10 nm and 15 nm following a phase transfer procedure with the capping agent 11-amino undecanoic acid (T_2 values recorded at 3 T) the r_2 value was found to be equal to 110.9 mM^{-1} s^{-1}, 169.9 mM^{-1} s^{-1} and 301.8 mM^{-1} s^{-1}, respectively.[22] Also, Yang *et al.*[31] by employing additional amphiphilic surfactants (anionic, cationic and neutral) through hydrophobic interactions around CoO MNPs, observed different r_2 values which is associated with the different structure of the coatings (T_2 values recorded at 0.5 T). Moreover, the presented values herein are much higher compared to γ-Fe_2O_3 MNPs as r_2 values increased from 13 to 64 mM^{-1} s^{-1}, with respect to the decreasing thickness of the silica layer;[36] values were determined using a 500 MHz NMR spectrometer.

Conclusions

The use of MNPs for new biomedical applications requires aqueous dispersion and further functionalization. Thus, tailoring the surface and understanding the surface characteristics are necessary. In the present work, we took advantage of hydrophobically modified water-soluble polymers, HMWSPs, to achieve these prerequisites in the case of hydrophobic MNPs. These HMWSPs, comprised of a poly(sodium methacrylate) or poly(sodium acrylate) backbone and pendent dodecyl methacrylate or dodecyl acrylamide chains, respectively, were synthesized by copolymerization or "grafting-to" methodologies. As a consequence of their amphiphilic character, these copolymers self-organize in aqueous media, forming supramolecular micellar structures above the critical micelle

concentration (CMC), while they are molecularly dissolved in water below CMC. The micellar structures are characterized by a high polydispersity in size due to the broad molecular weight distribution and the random architecture of the HMWSPs. In fact, for most polymers, single polymer chains, simple micelles and large-compound micelles were detected by DLS, while the latter two populations were also visualized by TEM. Moreover, it is shown that the crucial factor controlling CMC is the hydrophobic content and not the molar mass of the copolymers.

The hydrophobic $CoFe_2O_4$@OAm MNPs (9.4 nm) were successfully encapsulated into the hydrophobic cores of the micellar structures of the copolymers above CMC, forming $CoFe_2O_4$@HMWSP nanohybrids which are well stabilized in water by the hydrophilic backbones of the HMWSPs. To the best of our knowledge, such studies have been scarcely reported in the literature. Moreover, a representative example of $CoFe_2O_4$@HMWSP nanohybrids, $CoFe_2O_4$@P(ANa-co-DAAm), exhibited a sufficiently large r_2 value (313.6 mM^{-1} s^{-1}), making the HMWSP-mediated stabilization of hydrophobic MNPs an attractive technique for the preparation of potential T_2-contrast agents. Finally, the chemical composition of the synthesized amphiphilic polymers can be tailored, allowing fine-tuning of the properties of the MNPs@HMWSP nanohybrids that would lead to multi-responsive/multi-sensing water-dispersible MNPs@HMWSP nanohybrids.

Acknowledgements

This research was co-financed by the European Union (European Social Fund-ESF) and Greek national funds through the Operational Program "Education and Lifelong Learning" of the National Strategic Reference Framework (NSRF)-Research Funding Program: THALES. Investing in knowledge society through the European Social Fund. The authors thank Dr Maria Kollia from the Lab of Electron Microscopy and Microanalysis at the University of Patras for the TEM images.

References

1 (*a*) S. E. Webber, *J. Phys. Chem. B*, 1998, **102**, 2618–2626; (*b*) K. Kataoka, A. Harada and Y. Nagasaki, *Adv. Drug Delivery Rev.*, 2001, **47**, 113–131; (*c*) G. Riess, *Prog. Polym. Sci.*, 2003, **28**, 1107–1170; (*d*) J.-F. Gohy, *Adv. Polym. Sci.*, 2005, **190**, 65–136; (*e*) A. Blanazs, S. P. Armes and A. J. Ryan, *Macromol. Rapid Commun.*, 2009, **30**, 267–270.

2 (*a*) N. Hadjichristidis, M. Pitsikalis and H. Iatrou, *Adv. Polym. Sci.*, 2005, **189**, 1–124; (*b*) H. Cui, Z. Chen, S. Zhong, K. L. Wooley and D. J. Pochan, *Science*, 2007, **317**, 647–650; (*c*) A. E. Smith, X. Xu and C. L. McCormick, *Prog. Polym. Sci.*, 2010, **35**, 45–93; (*d*) Y. Mai and A. Eisenberg, *Chem. Soc. Rev.*, 2012, **41**, 5969–5985; (*e*) A. M. Budgin, Y. A. Kabachii, Z. B. Shifrina, P. M. Valetsky, S. S. Kochev, B. D. Stein, A. Malyutin and L. M. Bronstein, *Langmuir*, 2012, **28**, 4142–4151.

3 (*a*) C. Q. Wang, G. T. Li and R. R. Guo, *Chem. Commun.*, 2005, 3591–3593; (*b*) R. C. W. Liu, A. Pallier, M. Brestaz, N. Pantoustier and C. Tribet, *Macromolecules*, 2007, **40**, 4276–4286; (*c*) T. Kawata, A. Hashidzume and T. Sato, *Macromolecules*, 2007, **40**, 1174–1180; (*d*) Y. Li, Y. Zhang, D. Yang, C. Feng, S. Zhai, J. Hu, G. Lu and X. Huang, *J. Polym. Sci., Part A: Polym. Chem.*, 2009, **47**, 6032–6043; (*e*) Y. Ogata, M. Iwano, T. Mogi and Y. Makita, *J. Polym. Sci., Part B: Polym. Phys.*, 2011, **49**, 1651–1659.

4 (*a*) K. T. Wang, I. Iliopoulos and R. Audebert, *Polym. Bull.*, 1988, **20**, 577–582; (*b*) J. E. Klijn, J. Kevelam and J. B. F. N. Engberts, *J. Colloid Interface Sci.*, 2000, **226**, 76–82.

5 (*a*) F. Candau and J. Selb, *Adv. Colloid Interface Sci.*, 1999, **79**, 149–172; (*b*) L. Guillaumont, G. Bokias and I. Iliopoulos, *Macromol. Chem. Phys.*, 2000, **201**, 251–260; (*c*) K. Podhajecka, K. Prochazka and D. Hourdet, *Polymer*, 2007, **48**, 1586–1595.

6 (*a*) M. F. Francis, M. Piredda and F. M. Winnik, *J. Controlled Release*, 2003, **93**, 59–68; (*b*) E. Rotureau, E. Marie, E. Dellacherie and A. Durand, *Colloid Surf., A*, 2007, **301**, 229–238; (*c*) E. V. Korchagina and O. E. Philippova, *Langmuir*, 2012, **28**, 7880–7888; (*d*) R. Covis, C. Ladaviere, J. Desbrieres, E. Marie and A. Durand, *Carbohydr. Polym.*, 2013, **95**, 360–365.

7 J. Kötz, S. Kosmella and T. Beitz, *Prog. Polym. Sci.*, 2001, **26**, 1199–1232.

8 (*a*) O. E. Philippova and A. R. Khokhlov, *Petrol. Chem.*, 2010, **50**, 266–270; (*b*) D. A. Z. Wever, F. Picchioni and A. A. Broekhius, *Prog. Polym. Sci.*, 2011, **36**, 1558–1628.

9 (*a*) T. Osaka, T. Matsunaga, T. Nakanishi, A. Arakaki, D. Niwa and H. Iida, *Anal. Bioanal. Chem.*, 2006, **384**, 593–600; (*b*) J. L. Corchero and A. Villaverde, *Trends Biotechnol.*, 2009, **27**, 468–476; (*c*) S. A. Corr, Y. P. Rakovich and Y. K. Gun'ko, *Nanoscale Res. Lett.*, 2008, **3**, 87–104.

10 (*a*) Y. Wang, C. Xu and H. Ow, *Theranostics*, 2013, **3**, 544–560; (*b*) H. M. Joshi, *J. Nanopart. Res.*, 2013, **15**, 1235.

11 (*a*) X. Jia, D. Chen, X. Jiao, T. He, H. Wang and W. Jiang, *J. Phys. Chem. C*, 2009, **112**, 911–917; (*b*) D. Peddis, F. Orrù, A. Ardu, C. Cannas, A. Musinu and G. Piccaluga, *Chem. Mater.*, 2012, **24**, 1062–1071.

12 R. A. Sperling and W. J. Parak, *Philos. Trans. R. Soc. London, Ser. A*, 2010, **368**, 1333–1383.

13 (*a*) H. Ai, C. Flask, B. Weinberg, X. Shuai, M. D. Pagel, D. Farrell, J. Duerk and J. Gao, *Adv. Mater.*, 2005, **17**, 1949–1952; (*b*) B.-Su. Kim, J.-M. Qiu, J.-P. Wang and T. A. Taton, *Nano Lett.*, 2005, **5**, 1987–1991; (*c*) S. Lecommandoux, O. Sandre, F. Checot, J. Rodriguez-Hernandez and R. Perzynski, *Adv. Mater.*, 2005, **17**, 712–718; (*d*) S. Lecommandoux, O. Sandre, F. Checot and R. Perzynski, *Prog. Solid State Chem.*, 2006, **34**, 171–179; (*e*) J. Yang, E.-K. Lim, H. J. Lee, J. Park, S. C. Lee, K. Lee, H.-G. Yoon, J.-S. Suh, Y.-M. Huh and S. Haam, *Biomaterials*, 2008, **29**, 2548–2555; (*f*) A. Bakandritsos, G. Mattheolabakis, R. Zboril, N. Bouropoulos, J. Tucek,

D. G. Fatouros and K. Avgoustakis, *Nanoscale*, 2010, **2**, 564–572; (*g*) S. Mahajan, V. Koul, V. Choudhary, G. Shishodia and A. C. Bharti, *Nanotechnology*, 2013, **24**, 015603; (*h*) D.-H. Kim, E. A. Vitol, J. Liu, S. Balasubramanian, D. J. Gosztola, E. E. Cohen, V. Novosad and E. A. Rozhkova, *Langmuir*, 2013, **29**, 7425–7432.

14 (*a*) E. V. Shtykova, X. Huang, X. Gao, J. C. Dyke, A. L. Schmucker, B. Dragnea, N. Remmes, D. V. Baxter, B. Stein, P. V. Konarev, D. I. Svergun and L. M. Bronstein, *J. Phys. Chem. C*, 2008, **112**, 16809–16817; (*b*) L. M. Bronstein, E. V. Shtykova, A. Malyutin, J. C. Dyke, E. Gunn, X. Gao, B. Stein, P. V. Konarev, B. Dragnea and D. I. Svergun, *J. Phys. Chem. C*, 2010, **114**, 21900–21907; (*c*) X. Li, H. Li, G. Liu, Z. Deng, S. Wu, P. Li, Z. Xu, H. Xu and P. K. Chu, *Biomaterials*, 2012, **33**, 3013–3024; (*d*) E. Peng, E. S. G. Choo, Y. Sheng and J. M. Xue, *New J. Chem.*, 2013, **37**, 2051–2060.

15 V. Georgiadou, C. Kokotidou, B. Le Droumaguet, B. Carbonnier, T. Choli-Papadopoulou and C. Dendrinou-Samara, *Dalton Trans.*, 2014, **43**, 6377–6388.

16 Y. Tian, B. Yu, X. Li and K. Li, *J. Mater. Chem.*, 2011, **21**, 2476–2481.

17 L. I. Cabrera, A. Somoza, J. F. Marco, C. J. Serna and M. P. Morales, *J. Nanopart. Res.*, 2012, **14**, 873.

18 (*a*) A. G. Roca, S. Veintemillas-Verdaguer, M. Port, C. Robic, C. J. Serna and M. P. Morales, *J. Phys. Chem. B*, 2009, **113**, 7033–7039; (*b*) A. Ruiz, G. Salas, M. Calero, Y. Hernandez, A. Villanueva, F. Herranz, S. Veintemillas-Verdaguer, E. Martinez, D. F. Barber and M. P. Morales, *Acta Biomater.*, 2013, **9**, 6421–6430.

19 A. Patterson, *Phys. Rev.*, 1939, **56**, 978–982.

20 E. F. Kneller and F. E. Luborsky, *J. Appl. Phys.*, 1963, **34**, 656–658.

21 I. Sharifi, H. Shokrollahi, M. M. Doroodmand and R. Safi, *J. Magn. Magn. Mater.*, 2012, **324**, 1854–1861.

22 H. M. Joshi, Y. P. Lin, M. Aslam, P. V. Prasad, E. A. Schultz-Sikma, R. Edelman, T. Meade and V. P. Dravid, *J. Phys. Chem. C*, 2009, **113**, 17761–17767.

23 D.-H. Kima, H. Zeng, T. C. Ng and C. S. Brazel, *J. Magn. Magn. Mater.*, 2009, **321**, 3899–3904.

24 M. Y. Rafique, L. Pan, Q. Javed, M. Z. Iqbal and L. Yang, *J. Nanopart. Res.*, 2012, **14**, 1189.

25 J. Mohapatra, A. Mitra, D. Bahadur and M. Aslam, *CrystEngComm*, 2013, **15**, 524–532.

26 E. Solano, L. Perez-Mirabet, F. Martinez-Julian, R. Guzman, J. Arbiol, T. Puig, X. Obradors, R. Yanez, A. Pomar, S. Ricart and J. Ros, *J. Nanopart. Res.*, 2012, **14**, 1034.

27 M. Milnera, M. Stepanek, I. Zuskova and K. Prochazka, *Int. J. Polym. Anal. Charact.*, 2007, **12**, 23–33.

28 B. D. Ermi and E. J. Amis, *Macromolecules*, 1998, **31**, 7378–7384.

29 J. Yao, P. Ravi, K. C. Tam and L. H. Gan, *Langmuir*, 2004, **20**, 2157–2163.

30 J.-H. Lee, J.-T. Jang, J.-S. Choi, S. H. Moon, S.-H. Noh, J.-W. Kim, J.-G. Kim, I.-S. Kim, K. I. Park and J. Cheon, *Nat. Nanotechnol.*, 2011, **6**, 418–422.

31 H. Yang, H. Zhou, C. Zhang, X. Li, H. Hu, H. Wu and S. Yang, *Dalton Trans.*, 2011, **40**, 3616–3621.

32 Y. Xu, Y. Qin, S. Palchoudhury and Y. Bao, *Langmuir*, 2011, **27**, 8990–8997.

33 S. Tong, S. Hou, Z. Zheng, J. Zhou and G. Bao, *Nano Lett.*, 2010, **10**, 4607–4613.

34 Z. P. Chen, Y. Zhang, S. Zhang, J. G. Xia, J. W. Liu, K. Xu and N. Gu, *Colloid Surf.*, 2008, **316**, 210–216.

35 M. Menelaou, K. Georgoula, K. Simeonidis and C. Dendrinou-Samara, *Dalton Trans.*, 2014, **43**, 3626–3636.

36 S. L. C. Pinho, G. A. Pereira, P. Voisin, J. Kassem, V. Bouchaud, L. Etienne, J. A. Peters, L. Carlos, S. Mornet, C. F. G. C. Geraldes, J. Rocha and M.-H. Delville, *ACS Nano*, 2010, **4**, 5339–5349.